23.2: An Efficient Stacked OLED with Double-Sided Light Emission

J. X. Sun, X. L. Zhu, Z. G. Meng, X. M. Yu, M. Wong and H. S. Kwok

Center for Display Research and Dept. of Electrical and Electronic Engineering,

The Hong Kong University of Science and Technology, Clear Water Bay, Kowloon, Hong Kong

Abstract

An efficient double-sided emitting OLED employing a stacked geometry has been fabricated. It uses a reflective composite silver electrode as the middle reflective layer. It can be used in a passive matrix (PM) driving scheme with independent control of both displays. Superior electroluminescent (EL) performance of the OLED on both ("bottom" and "top") sides can be easily achieved without interference independently. The power efficiencies at 100 cd/m^2 of bottom- and top-emitting OLEDs are 10.3 lm/W and 12.1 lm/W, respectively.

1. Introduction

Double-sided emission organic light-emitting diodes (OLED) utilizing transparent cathode technology have been proposed and demonstrated in recent years [1-4]. However, the images displaying on both sides are actually the same and are mirror images of each other. Therefore, the applications of such displays are rather limited. For many situations, independent images on both sides are required. Recently some progress has been made in this problem, e.g., Ko et al [5] reported a 1.5-inch full color double-sided active matrix OLED (AMOLED), in which independent images on each side can be displayed. However, the bottom- and top-emitting OLEDs are laterally displaced on one substrate, hence resulting in a reduced spatial resolution. A double-sided emission stacked OLEDs have also been demonstrated [6]. In this display, an intermediate reflective Al:Nd alloy (Al: Nd=98: 2) electrode is employed as the common cathode. This necessitated the construction of an "inverted" top-emitting OLED that is generally less efficient than a "non-inverted" OLED, although superior electron injection material of 2,5-bis(6'-(2'-2''-bipyridyl))-1,1-dimethyl-3,4-diphenylsilole [7] and hole injection layer of MoO_3 [8, 9] were used in their experiment.

In this paper, we propose to use a "bipolar" composite silver electrode in a stacked organic light-emitting diode (SOLED) capable of emitting light on both sides. This bipolar layer can act as the anode to one OLED and as the cathode to the other. Thus both OLEDs can be of the normal non-inverted type. The bipolar electrode used here is consisting of a thermally evaporated stack of LiF(1nm)/Al(3nm)/Ag(70nm) followed by a carbon tetrafluoride (CF_4) plasma treatment. Compared (Table I) to the previously reported bipolar electrodes, the proposed electrode is superior either in its simpler construction or its better performance.

As an example, we fabricated a SOLED with double-sided green light emission. The structures of this device together with the detailed parameters are shown in Fig. 1. The bottom-and top-emitting OLED can be individually controlled to better performance without affecting each other. In addition, an internal circuit diagram of passive matrix (PM) OLED display using double-sided emission SOLED as pixels are proposed.

Table I. Comparison of different kinds of "bipolar" electrode

	As cathode	As anode	Thermal evaporation or Sputtering?
Mg:Ag/ITO [10]	Good	Good	Both
CuPc/ITO/CuPc [11]	Not good	Good	Both
Mg:Ag/IZO [12]	Good	Good	Both
LiF/Al/Au [13]	Good	Not good	Thermal evaporation Only
LiF/Al/Ag (This paper)	Good	Very good	Thermal evaporation Only

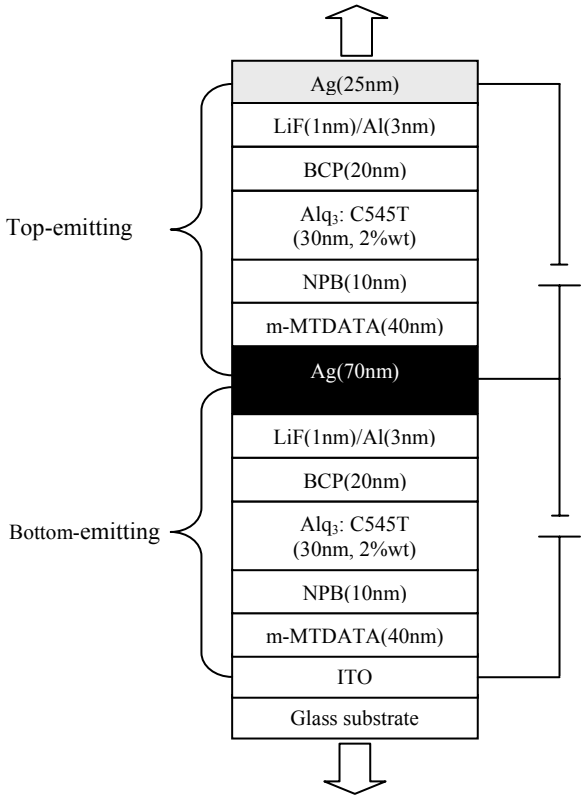

Fig. 1 Device structure of a SOLED with double-sided green light emission

ISSN0006-0966X/06/3702-1193-$1.00+.00 © 2006 SID

2. Experimental Details

The SOLED were fabricated on 75nm-ITO coated glass with a sheet resistance of 25Ω/□. The detailed cleaning procedures of substrates are the same with and can be referred to the previous report [13]. Organic materials including 4,4',4"-tris(N-3-methylphenyl-N-phenyl-amino)-triphenylamine (m-MTDATA); N,N' -di(naphthalene-1-yl)-N,N' -diphenyl-benzidine (NPB); tris(8-hydroxyquinoline) aluminium(III) (Alq_3); 10-(2-benzothia zolyl) - 1,1,7,7-tetramethyl-2,3,6,7-tetrahydro 1H,5H,11H - benzo[1]pyrano[6,7,8-ij]quinolizin-11-one (C545T) and 2,9-Dimethyl-4,7-diphenyl-1,10-phenanthroline (BCP) were all used as received (from LumTec Corp.) without further purification. Prior to deposition of organic films, the ITO were treated by CF_4-Plasma at 20 Pa for 10 seconds to improve hole-injection ability [14]. Then the constituent organic layers were formed sequentially by thermal evaporation in a high vacuum chamber with the base pressure lower than 10^{-6} Torr. The typical deposition rate of organic thin films was 0.15nm/s, which was monitored by quartz oscillators *in situ*

Next, the samples were transferred to another vacuum chamber for middle electrode preparation. LiF(1nm), Al(3nm) and Ag(70nm) were thermally evaporated in sequence with respective deposition rates of 0.03, 0.2 and 0.3 nm/s. The device active area was therefore decided by the pattern of the middle electrode, which was defined by a shadow mask. Then, the samples were treated with CF_4 plasma again under the same conditions as before. Interestingly, this treatment makes the silver surface morphology better as well. Fig. 2 shows the atomic force microscope (AFM) images of the middle electrode before and after treatment. Mean roughness of 1.66nm and 1.37nm were obtained for non-treated and treated samples, respectively.

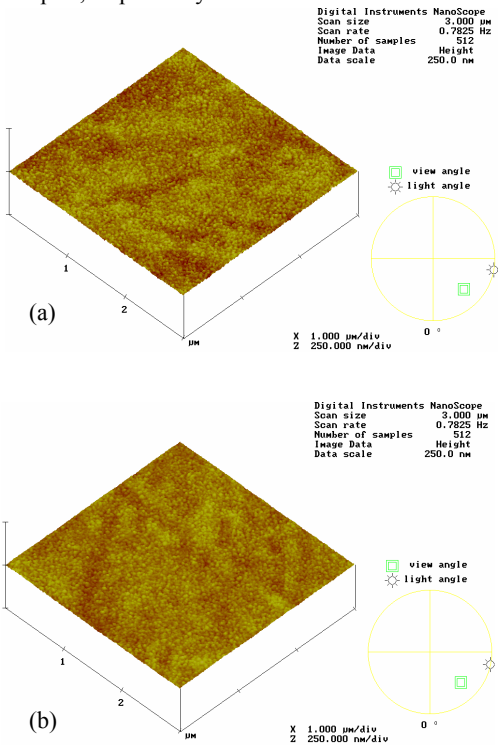

Fig. 2 Surface morphologies of middle electrode (a) before and (b) after CF_4-plasma treatment

The whole stack was completely finished with the "non-inverted" top-emitting OLED preparation on top of the middle electrode with the same structure as the bottom one except that the topmost silver layer was semitransparent for achieving better light out-coupling efficiency [15]. The bottom ITO anode, middle composite silver electrode and top semitransparent cathode can be individually connected to external power lines so as to measure separately the EL performance of bottom- and top-emitting OLED. The luminance-current density - voltage (L-J-V) characteristics of the devices were recorded simultaneously with a semiconductor parameter analyzer (HP4145B) combined with a calibrated silicon photodiode mounted above the device. The electroluminescent (EL) spectra were obtained using a PhotoResearch PR650 spectrometer. All measurements were carried out under ambient atmosphere without device encapsulation.

3. Results and discussion

With the configuration of SOLED shown in Fig.1, we obtained excellent EL performance. Fig. 3 shows a comparison of luminance versus voltage (L-V) characteristics between the top- and bottom-emitting OLED in one SOLED. It can be seen that they both turn on at about 3V, and reach 100 cd/m^2 at ~ 4.5 V. At higher voltages, the top-emitting OLED shows better L-V characteristics than the bottom-emitting one. This is attributed to out-coupling enhancement due to the microcavity structure [15]. Further evidence can be found in the EL spectra comparison as shown in Fig. 4. It is clearly seen that the narrower full width at half of maximum height (FWMH) was obtained for top-emitting device. The CIE coordinates of bottom- and top-emission are also denoted for reference. The stronger microcavity effect for the top-emitting OLED will produce narrower FWMH, better color purity and better efficiency [16].

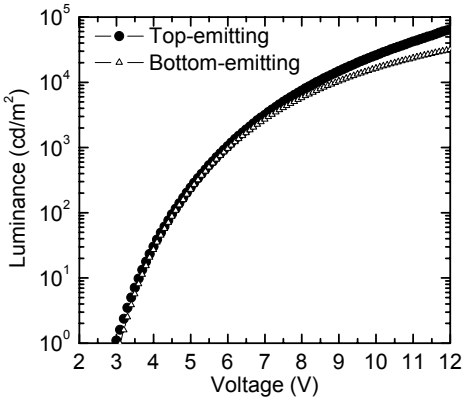

Fig. 3 L-V characteristics of top- and bottom-emitting OLED in a SOLED

Figs. 5 (a) and (b) show a comparison of luminous efficiency and power efficiency of the two devices in the SOLED. At 20mA/cm^2, the luminous efficiency of top- and bottom-emitting OLED are 18.5 and 16.8 cd/A, respectively. Theoretically, the microcavity device shall have doubled efficiency of non-cavity device [17]. Therefore, luminous efficiency over 30 cd/A will be

expected on condition that the thicknesses of all functional layers are optimized. The power efficiency at 100 cd/m^2 and 1000 cd/m^2 are 12.1 and 9.9 lm/W, 10.3 and 8.6 lm/W for top- and bottom-emitting OLED, respectively. These EL characteristics are definitely suitable for display applications.

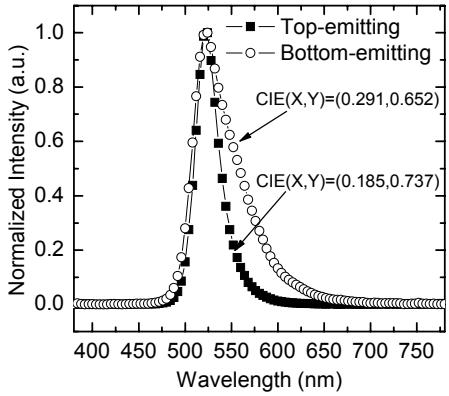

Fig. 4 EL spectra comparison of top- and bottom-emitting OLED in a SOLED

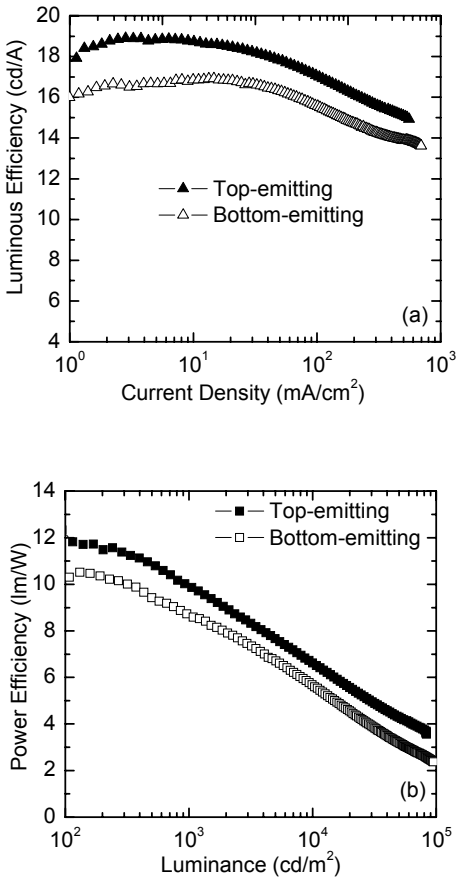

Fig. 5 (a) Luminous efficiency comparison; and (b) Power efficiency of top- and bottom-emitting OLED in a SOLED

4. Driving scheme

The double-side emitting SOLED can be driven so that the images on opposite sides can be independently controlled. By connecting the bottom-most and top-most electrodes of the SOLED in the fabrication process, the two OLEDs can be simply regarded as two anti-parallel diodes, as shown in Fig. 6. Based on this configuration, we can drive this double-sided SOLED in a passive matrix or active matrix manner.

Fig. 7 shows the schematic diagram of a PMOLED display. Such display comprises a plurality of scan lines Com1, Com2, Com3, Com4, Com5; a plurality of data lines Seg1, Seg2, Seg3, Seg4, Seg5; and a pixel array; wherein each pixel is a SOLED in which the top-emitting and bottom-emitting OLED are connected as shown in Fig. 6. Within one pixel, the middle electrode of SOLED has to be connected to one scan line and the outer most anode and cathode have to be connected together and connected to the corresponding data line. Positive and negative voltages interlaced together may be used to drive this PMOLED display. Selection and de-selection of a particular scan line is respectively achieved by putting a definite voltage on or putting in a high impedance state the port of the scan circuit to which the line is connected.

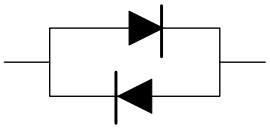

Fig. 6 Schematic diagram of the parallel diodes for each pixel in double sided emission PM/AMOLED display

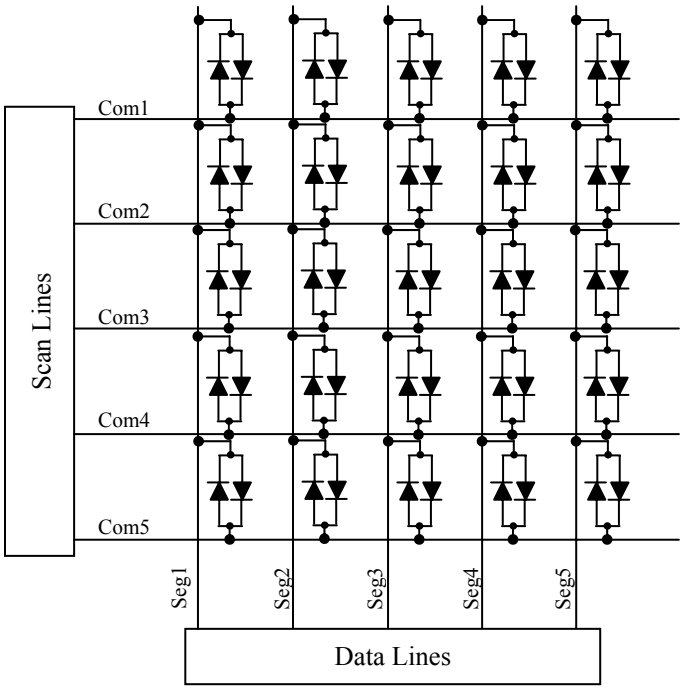

Fig. 7 Driving scheme of PMOLED display using double-sided emission SOLED as pixels

Apart from this PM driving scheme, this double-sided SOLED can also be driven as an AMOLED display. The driving method is also affected by positive and negative voltages and will be discussed elsewhere [18]. The present design may find applications in small size displays in folding-type geometry. It may also open up new areas of product design due to its capability of displaying two independent images.

5. Conclusion

In summary, we have successfully fabricated an efficient double-sided emitting stacked organic light-emitting diode utilizing a reflective composite silver electrode as the middle electrode. In particular, the properties and key roles of this "bipolar" electrode are characterized and emphasized. Based on this middle electrode, the power efficiency of green top- and bottom-emitting OLED with emitter of Alq_3: C545T are exceeding 10 lm/W at the same time with a luminance of 100 cd/m^2. Further, we have proposed driving schemes for this double-sided emission PMOLED display. This new type of double-sided emission SOLED may be used as pixels in AMOLED as well. They will find applications in folding-type displays as well as in new applications where independent control of images on both sides is needed.

This research was supported by the Hong Kong Government Innovations and Technology Fund.

6. References

[1] G. Gu, V. Bulovic, P. E. Burrows, S. R. Forrest, and M. E.Thompson, *Appl. Phys. Lett.,* **68**, 2606 (1996).

[2] G. Parthasarathy, P. E. Burrows, V. Khalfin, V. G. Kozlov, and S. R. Forrest, *Appl. Phys. Lett.,* **72**, 2138 (1998).

[3] K. H. Lee, S. Y. Ryu, J. H. kwon, S. W. Kim, H. K. Chung, *SID Symposium Digest,* **34**, 104 (2003).

[4] X. Liu, D. Poitras, Y. Tao, and C. Py, *J. Vac. Sci. Technol. A,* **22**, 764 (2004).

[5] C. W. Ko, S. H. Hu, S. H. Li, T. H. Hsiao, K. S. Lee, C. J. Chen, and J. J. Lih, *SID Symposium Digest,* **36**, 961 (2005).

[6] T. Miyashita, S. Naka, H. Okada, and H. Onnagawa, *Jpn. J. Appl. Phys.* Vol. **44**, No. 6A, 3682 (2005).

[7] S. Tabatake, S. Naka, H. Okada, H. Onnagawa, M. Uchida, T. Nakano, and K. Furukawa, *Jpn. J. Appl. Phys.* Vol. **41**, 6582 (2002).

[8] S. Tokito, K. Noda, and Y. Taga, *J. Phys. D*, **29**, 2750 (1996).

[9] K. J. Reynolds, J. A. Barker, N. C. Greenham, R. H. Friend, G. L. Frey, *J. Appl. Phys.,* **92**, 7556 (2002).

[10] P. E. Burrows, S. R. Forrest, S. P. Sibley, and M. E. Thompson, *Appl. Phys. Lett.,* **69**, 2959, (1996).

[11] G. Gu, G. Parthasarathy, and S. R. Forrest, *Appl. Phys. Lett.,* **74**, 305, (1999).

[12] S. Tanaka and C. Hosakawa, *U. S. Patent* No. 6,107,734 August 22, (2000).

[13] J. X. Sun, X. L. Zhu, H. J. Peng, M. Wong, and H. S. Kwok, *Appl. Phys. Lett.,* **87**, 093504 (2005).

[14] H. J. Peng, X. L. Zhu, J. X. Sun, Z. L. Xie, S. Xie, M. Wong, and H. S. Kwok, *Appl. Phys. Lett.,* **87**, 173505 (2005).

[15] H. J. Peng, J. X. Sun, X. L. Zhu, X. M. Yu, M. Wong, and H. S. Kwok, *Appl. Phys. Lett.,* **88**, 073517 (2006).

[16] S. F. Hsu, C. C. Lee, S. W. Hwang, and C. H. Chen, *Appl. Phys. Lett.,* **86**, 253508, (2005).

[17] C. L. Lin, H. W. Lin, and C. C. Wu, *Appl. Phys. Lett.,* **87**, 021101 (2005).

[18] J. X. Sun, X. L. Zhu, Z. G. Meng, M. Wong, and H. S. Kwok, (unpublished).